Journal of Geophysical Research: Space Physics

RESEARCH ARTICLE
10.1029/2018JA025334

The Ionospheric Impact of an ICME-Driven Sheath Region Over Indian and American Sectors in the Absence of a Typical Geomagnetic Storm

Diptiranjan Rout[1], D. Chakrabarty[1], S. Sarkhel[2], R. Sekar[1], B. G. Fejer[3], G. D. Reeves[4], Atul S. Kulkarni[5], Nestor Aponte[6], Mike Sulzer[6], John D. Mathews[7], Robert B. Kerr[8], and John Noto[8]

[1]Physical Research Laboratory, Ahmedabad, India, [2]Indian Institute of Technology Roorkee, Roorkee, India, [3]Utah State University, Logan, UT, USA, [4]Los Alamos National Laboratory, Los Alamos, NM, USA, [5]Indian Institute of Geomagnetism, Navi Mumbai, India, [6]Space and Atmospheric Science Arecibo Observatory, Arecibo, Puerto Rico, [7]The Pennsylvania State University, State College, PA, USA, [8]Computational Physics Inc., Springfield, VA, USA

Abstract On 13 April 2013, the ACE spacecraft detected arrival of an interplanetary shock at 2250 UT, which is followed by the passage of the sheath region of an interplanetary coronal mass ejection (ICME) for a prolonged (18-hr) period. The polarity of interplanetary magnetic field Bz was northward inside the magnetic cloud region of the ICME. The ring current (SYM-H) index did not go below −7 nT during this event suggesting the absence of a typical geomagnetic storm. The responses of the global ionospheric electric field associated with the passage of the ICME sheath region have been investigated using incoherent scatter radar measurements of Jicamarca and Arecibo (postmidnight sector) along with the variations of equatorial electrojet strength over India (day sector). It is found that westward and eastward prompt penetration (PP) electric fields affected ionosphere over Jicamarca/Arecibo and Indian sectors, respectively, during 0545–0800 UT. The polarities of the PP electric field perturbations over the day/night sectors are consistent with model predictions. In fact, DP2-type electric field perturbations with ~40-min periodicity are found to affect the ionosphere over both the sectors for about 2.25 hr during the passage of the ICME sheath region. This result shows that SYM-H index may not capture the full geoeffectivenss of the ICME sheath-driven storms and suggests that the PP electric field perturbations should be evaluated for geoeffectiveness of ICME when the polarity of interplanetary magnetic field Bz is northward inside the magnetic cloud region of the ICME.

Key Points:
- Effects of ICME sheath region is observed on equatorial ionosphere in the absence of a typical storm
- Prompt penetration electric field can capture the geoeffectiveness of an ICME event
- The geoeffectivenss of an ICME can be efficiently evaluated by the PP/OS electric field effects on the global ionosphere

Correspondence to:
D. Rout,
diptir@prl.res.in

Citation:
Rout, D., Chakrabarty, D., Sarkhel, S., Sekar, R., Fejer, B. G., Reeves, G. D., et al. (2018). The ionospheric impact of an ICME-driven sheath region over Indian and American sectors in the absence of a typical geomagnetic storm. *Journal of Geophysical Research: Space Physics*, *123*. https://doi.org/10.1029/2018JA025334

Received 8 FEB 2018
Accepted 24 APR 2018
Accepted article online 9 MAY 2018

1. Introduction

A coronal mass ejection (CME) in an interplanetary (IP) medium is called an *interplanetary CME* or *ICME*. Magnetic cloud (MC) is an important subset of ICME wherein the magnetic field is enhanced and rotates slowly through a large angle. In addition, proton temperature is low inside a MC structure and as a consequence, plasma beta is usually less than 1 (e.g., Burlaga et al., 1982; Zurbuchen & Richardson, 2006). Another important feature of an ICME is a sheath region formed ahead of it and bounded by the shock front of the ICME. The plasma in an ICME sheath region is highly compressed and turbulent. The ICME sheath is generally characterized by enhanced and fluctuating magnetic fields, proton density, velocity, dynamic pressure, and temperature. The ICME sheath region can drive space weather events (e.g., Gopalswamy et al., 2008; Lugaz et al., 2016; Tsurutani et al., 1988). Huttunen and Koskinen (2004) found that the postshock streams and sheath regions are the causes for intense magnetic storms and strong high-latitude activity. In fact, the ICME-driven IP shock can accelerate solar wind particles to energies of hundreds of MeV on many occasions and this acceleration process strongly depends on the geometry of the shock and the structure of the sheath region (Manchester et al., 2005).

It is to be noted that both the sheath and MC regions of an ICME can drive (e.g., Echer et al., 2008; Huttunen et al., 2006; Tsurutani et al., 1988) geomagnetic storms although several studies suggest fundamental differences in the response of the magnetosphere-ionosphere system for sheath and MC-driven geomagnetic storms. Huttunen et al. (2006) showed that the asymmetry in the ring current intensity develops during the passage of sheath and MC domains of ICMEs. It was further suggested that the sheath-driven geomagnetic

storms cause larger morning/afternoon asymmetry in the ring current than MC-driven geomagnetic storms. It is argued that the sheath-driven geomagnetic storms show stronger auroral activity whereas the MC-driven geomagnetic storms show strong enhancement in ring current (Huttunen et al., 2002; Pulkkinen et al., 2007) although reasons for this are not fully understood till today. It is also not clear whether development of global plasma convection (DP2 current system) associated with a typical geomagnetic storm can occur without significant changes in the ring current. This is an important question in the context of the efficacy of Dst index to gauge geomagnetic storm intensity (e.g., Borovsky & Shprits, 2017).

During the passage of ICME sheath and MC regions at 1 AU, the Y-component (dawn-dusk) of interplanetary electric field (IEFy) can penetrate (Wei et al., 2011) nearly instantaneously from magnetosphere to low-latitude ionosphere as the response time of the shielding region (Alfven layer) at the inner edge of the ring current is relatively larger. On the other hand, if IEFy rapidly flips to dusk-dawn direction after staying in the dawn-dusk direction in a relatively stable manner for some time, an overshielding (OS) condition (e.g., Chakrabarty et al., 2006) is generated. At this time, the inner magnetosphere experiences the OS electric field (or the residual shielding field) that was generated to counter the PP electric field. The polarity of PP electric field is generally expected to be eastward till 2200 LT (e.g., Fejer et al., 2008; Nopper & Carovillano, 1978) and westward afterwards. As a consequence, the polarity of OS electric field is westward (e.g., Simi et al., 2012) during daytime and eastward (e.g., Chakrabarty et al., 2006) during nighttime. It is to be noted at this point that the shielding time constant is typically of the order of 20–30 min (e.g., Kikuchi et al., 2010; Senior & Blanc, 1984), which is closer to the periods (30–60 min) of DP2 fluctuations. Therefore, the changes at the inner edge of the ring current region that decide the shielding process during the global plasma convection associated with DP2 event can be complicated and require critical attention.

There exist very few studies on PP electric field over low-latitude-driven particularly by sheath region of an ICME. The work of Guo et al. (2011) showed that the effects of PP electric field over low latitude in daytime are associated with MC and sheath regions of ICME. In this case, an oscillatory ionospheric electric field was observed during the passage of a sheath region. It is also to be noted that the passage of sheath region caused the SYM-H to reach ~ -80 nT. In addition, Wei et al. (2011) found multiple electric field penetrations over dip equatorial ionosphere during a passage of an ICME sheath in daytime and a strong geomagnetic storm followed due to the passage of MC region that reduced SYM-H to less than -200 nT. It is important to mention here that most of the intense geomagnetic storms are mainly driven by the MC region as this region is generally associated with strong and steady southward IMF Bz. In the present study, the ICME event on 11 April 2013 is investigated. This ICME event is special as the MC region in this ICME was not geoeffective and did not drive any geomagnetic storm (SYM-H did not go below -7 nT) in contrast to the general scenario. However, the PP electric field is found to affect the global ionosphere during the passage of the sheath region of this ICME. Therefore, it is shown that the PP electric field perturbations (rather than the changes in the ring current indices or changes in SYM-H) should be evaluated for geoeffectiveness of ICME when the polarity of IMF Bz is northward inside MC.

2. Data Set

The solar wind parameters (like solar wind magnetic field, proton temperature, flow speed, proton density, solar wind dynamic pressure, and electric field) are taken from the NASA GSFC CDAWeb (http://cdaweb.gsfc.nasa.gov/) wherein solar wind parameters are corrected for propagation lag till the nose of the bow shock. The temporal resolution of solar wind parameters is 1 min. The indices like SYM-H (symmetric component of ring current), AL (westward auroral electrojet), AU (eastward auroral electojet), and PC index are taken from CDAweb with 1-min temporal resolution. The vertical plasma drift data over Jicamarca (latitude: 12°S, longitude: 76.8°W, dip angle: 0.8°) and Arecibo (latitude: 18.3° N, longitude: 67° W, dip angle: 45°, and magnetic latitude 30°N) are used for this investigation. Jicamarca is a dip equatorial station whereas Arecibo is a magnetically midlatitude station. This event was on a world day when both the incoherent scatter radar (ISR) radars were operated. In this work, Jicamarca drifts between 250 and 360 km are taken and in this altitude region, the drifts do not change much with altitude (e.g., Fejer, 2011). The maximum uncertainty in Jicamaraca radar observation is 5 m/s. The linear regularization technique applied in the Arecibo data introduces smoothing (Sulzer et al., 2005) of the drifts. Arecibo being a magnetically midlatitude station, the meridional wind velocity measured by a collocated Fabry-Perot interferometer, is also taken into consideration to delineate the plasma drift arising from electric field alone. The fitting error for the meridional winds is typically <2 m/s. The height integrated (256–404 km) perpendicular

north velocity is used for Arecibo along with the meridional wind measurements to infer the vertical plasma drift due to electric fields. The perpendicular north velocity (Vpn) is the plasma drift (E×B) perpendicular to north-south component of Earth's magnetic field (Fejer, 1993). As pointed out by Fejer and Emmert (2003), the typical accuracy of the Arecibo drifts at this altitude region is 10–20 m/s during nighttime. The horizontal magnetic field (H) variations of two Indian stations (Tirunelveli [TIR]: 8.7°N, 77.8°E, and dip angle 0.5°; Alibag [ABG]: 18.6°N, 72.9°E, and dip angle 26.4°) are used to deduce the equatorial electrojet (EEJ) strength. The temporal resolution of the ΔH data is 1 min. $\Delta H_{TIR} - \Delta H_{ABG}$ represents the difference in the variation in the horizontal component of geomagnetic field over an equatorial (TIR) and an off-equatorial (ABG) stations in the Indian sector, and the difference provides strength of EEJ. The EEJ strength can be used as a proxy for electric field variation over the dip equator in daytime (Rastogi & Patil, 1986). In order to identify the onset of substorm, if any during this event, the energetic electron flux measurements at geosynchronous altitude by Los Alamos National Laboratory (LANL) and GOES-13 satellites are considered. Six energy channels from LANL-01A and LANL-08 satellites (E1: 48–70 keV; E2: 69–102 keV; E3: 100–150 keV; E4: 145–220 keV, E5: 220–341 keV, E6: 341-490 keV) and four energy channels from GOES-13 (E1: 75 keV; E2: 150 keV; E3: 275 keV; E4: 475 keV) satellite are used in this present work.

3. Results

Figure 1 shows the observations of IP parameters at L1 point in GSM coordinate system and geomagnetic SYM-H index during 13–15 April 2013. The variation of (a) the X-component interplanetary magnetic field (IMF Bx in nT), (b) IMF By in nT, (c) IMF Bz in nT, (d) the total magnetic field intensity ($| B |$ in nT), (e) solar wind proton temperature (Tp in K), (f) solar wind velocity (Vp in km/s), (g) solar wind proton density (Np in cc^{-1}), (h) solar wind dynamic pressure (P in nPa), and (i) symmetric component of ring current (SYM-H in nT) are shown in Figure 1 (from top to bottom) during 13–15 April 2013 in UT. The arrival time of the ICME-driven IP shock is marked by vertical red line at 2250 UT on 13 April 2013. It is followed by a prolonged sheath region, which continues for ~18 hr. When the IP shock arrived at 2250 UT on 13 April 2013, the solar wind speed abruptly changed from 350 to 540 km/s, density from 3 to 12 cc^{-1}, and the dynamic pressure from 1 to 6 nPa. The sheath region of ICME is present between the two vertical dashed lines after 2250 UT on 13 April 2013 till 1735 UT on 14 April 2013. The sheath region is followed by a MC region. It can be clearly noticed that the solar wind magnetic field components were highly fluctuating in the sheath region. In contrast to the sheath region, the signatures of MC region can easily be identified from the decrease in solar wind density, dynamic pressure and the plasma temperature and sharp initial increase in magnetic field strength (~14 nT) followed by monotonic decrease. Interestingly, observations of SYM-H did not reveal the usual signatures of a typical geomagnetic storm as IMF Bz was predominately northward in the sheath region except during 0545–0800 UT on 14 April 2013.

Figure 2 presents the variations in IEFy and its responses during 0545–0800 UT on 14 April 2013 over polar, mid, and equatorial latitudes in addition to the meridional wind velocity over Arecibo. Figure 2 shows (a) propagation time lag corrected IEFy (in mV/m; following the methodology adopted in Chakrabarty et al., 2015), (b) variations in polar cap (PC) index over polar region, (c) averaged perpendicular north plasma drift (Vpn in m/s) over Arecibo (black line) along with its seasonal quiet time variations (in blue line) from Fejer (1993), (d) variations of meridional wind velocity (filled black triangles) over Arecibo obtained using Fabry-Perot interferometry, (e) ISR measured vertical plasma drift over Jicamarca (Vd in m/s) in black along with quiet time vertical drift (in blue line) from Scherliess and Fejer (1999), and (f) EEJ strength (EEJ in nT) over India in black on the top of which a quiet day (13 April 2013) EEJ variation in blue during 0000–1200 UT is overlaid. The *X*-axis (Figure 2f) is marked by universal time (UT) and the corresponding local times (LT) of different measurements are mentioned on the top of the *X*-axis in Figures 2c, 2e, and 2f for Arecibo, Jicamarca, and Tirunelveli, respectively. The gray shaded region shows the duration of penetration/OS of IEFy during 0545–0800 UT when the ICME-driven sheath region passes the Earth's orbit. It is to be noticed from subplots 2a and 2b that the variations in PC index over polar region goes hand in hand with the IEFy or dawn-dusk component of IEF during this interval. The PC index can be used as a proxy of the ionospheric electric field in the near-pole region (Troshichev et al., 2000). In order to know the prompt electric perturbation over geomagnetically midlatitude region (geographically low-latitude), the ISR measured perpendicular plasma drift over Arecibo has been taken along with meridional wind velocity (Figure 2d). It can be seen from Figure 2c that the perpendicular plasma drift is very different from the average quiet time plasma drift (marked with blue line). The perpendicular plasma drift is more downward during 0545–0800 UT (0115–0330 LT) when the

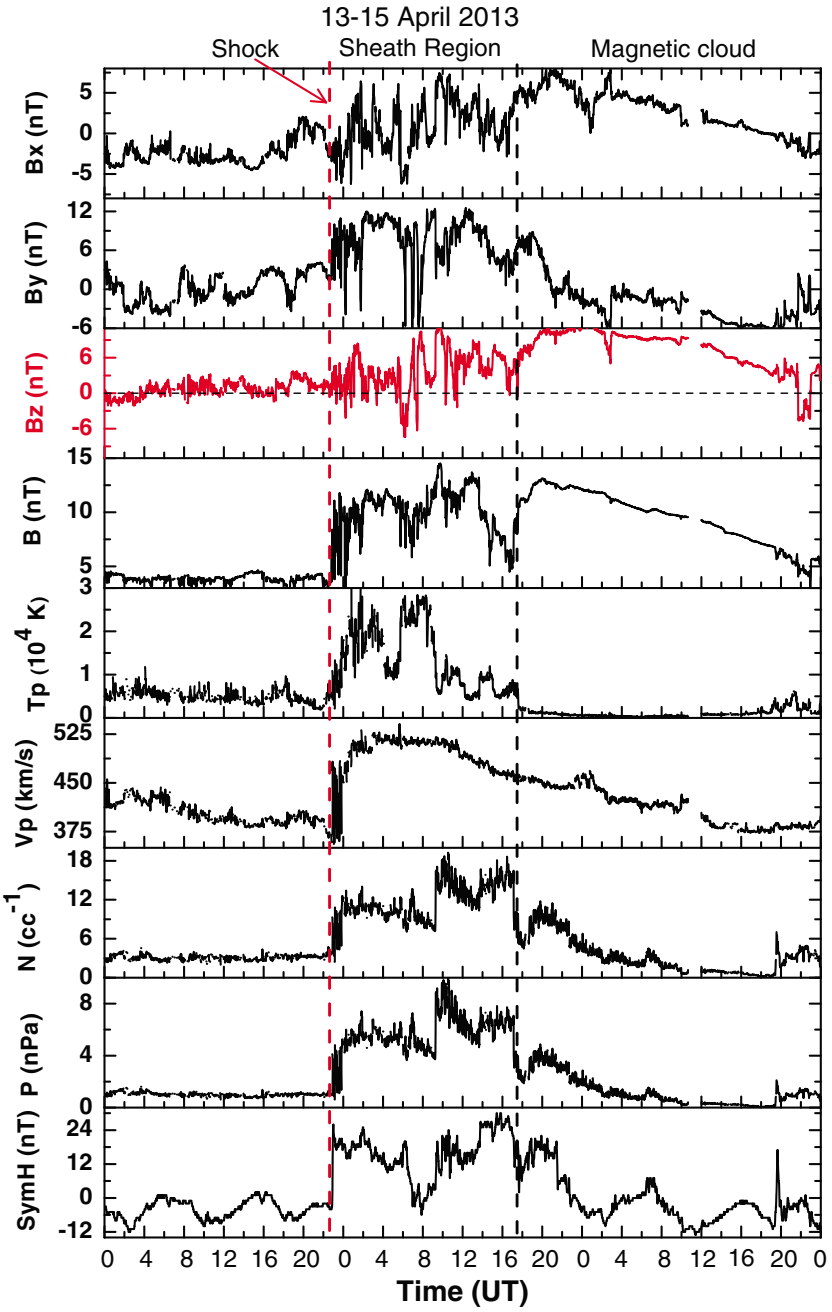

Figure 1. From top to bottom are the variation in (a) the X-component interplanetary magnetic field (IMF Bx in nT), (b) IMF By in nT, (c) IMF Bz in nT, (d) the total magnetic field intensity (| *B* | in nT), (e) solar wind proton temperature (Tp in K), (f) solar wind velocity (V in km/s), (g) solar wind proton density (Np in cc^{-1}), (h) solar wind dynamic pressure (P, in nPa), and (i) symmetric component of ring current (SYM-H in nT) during 13–15 April 2013 in UT. The arrival time of the CME-driven IP shock at 2250 UT on 13 April 2013 is marked by vertical red line. The sheath and magnetic cloud regions are also marked. CME = coronal mass ejection.

meridional wind velocity remains nearly constant (~ −20 m/s) and equatorward. The plasma drift has attained a minimum value of ~ −29 m/s at 0618 UT despite the presence of an equatorward wind suggesting a clear westward electric field perturbation. In the Figure 2e, the average quiet time drift over Jicamarca clearly suggests that the electric field is generally westward during nighttime. Thus, the sharp deviation from the nocturnal variations of vertical drift is the direct contribution from the PP electric field from high latitude to low latitude. A large downward plasma drift is observed during the interval 0545–0800 UT (0045–0300 LT), which is exactly opposite to the dawn-dusk component of IEF. The downward plasma drift changed from

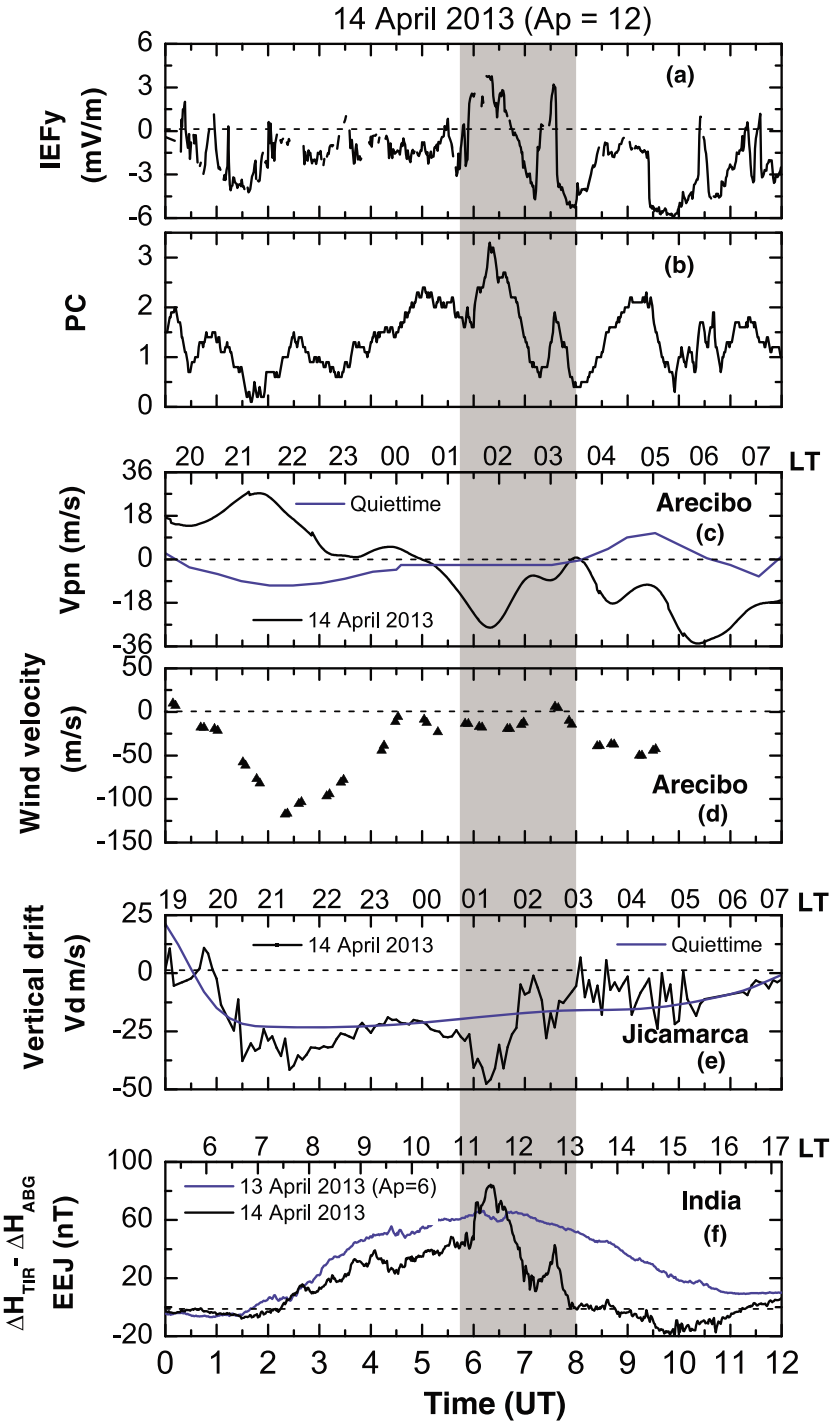

Figure 2. Variation in (a) propagation time lag corrected IEFy (in mV/m), (b) polar cap (PC) index, (c) averaged perpendicular north plasma drift (Vpn in m/s) over Arecibo along with seasonal quiet time variations (in blue line) from Fejer (1993), (d) variations of meridional wind velocity over Arecibo where the positive value indicates poleward and negative for equatorward, (e) ISR measured vertical plasma drift over Jicamarca (Vd in m/s) in black along with quiet time vertical drift (in blue line) from Scherliess and Fejer (1999) where the vertical drift is positive upward, and (f) equatorial electrojet strength (EEJ in nT) over India in black, which is overlaid with a quiet day (14 April 2013) EEJ variation in blue during 0000–1200 UT. The gray shaded region (0545–0800 UT) marks the interval when PP/OS electric field perturbations are seen over Arecibo/Jicamarca and Indian sector. IEF = interplanetary electric field.

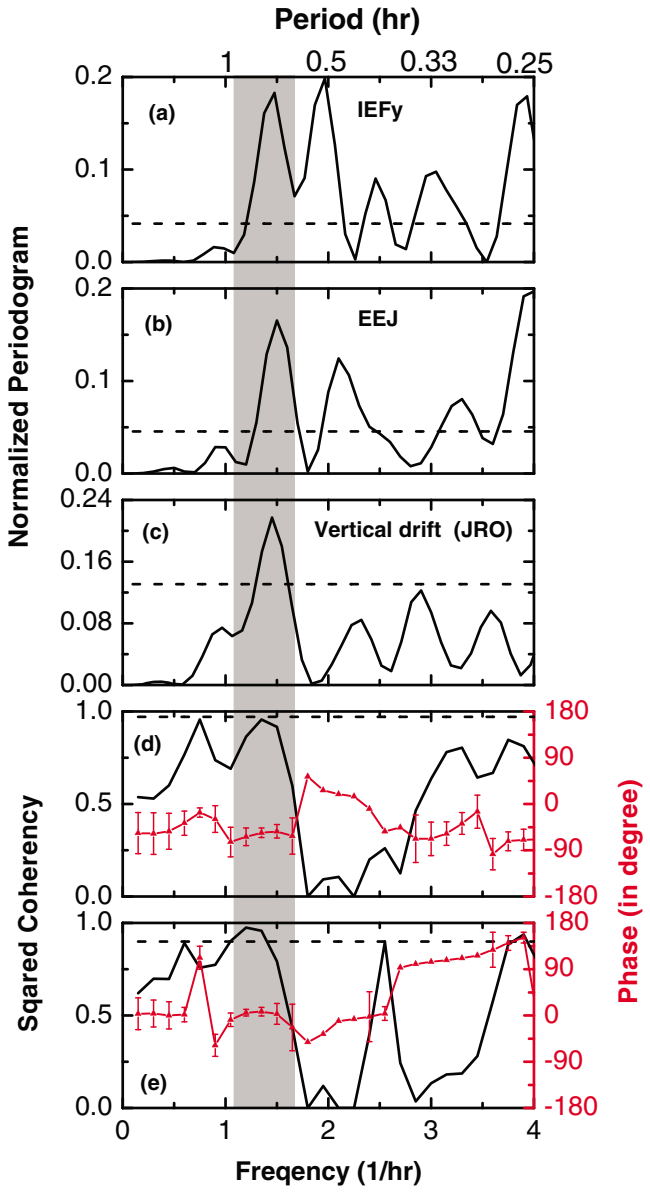

Figure 3. Harmonic analyses of (a) IEFy, (b) EEJ, and (c) vertical drift during the interval 0545–0800 UT. The dashed horizontal lines in Figures 3a–3c are marked at 5% significance level determined by Siegel's test. The squared coherency (black) and phase spectra (red) between IEFy and EEJ strength, and IEFy and vertical drift are depicted in Figures 3d and 3e respectively. The horizontal dashed line in Figures 3d and 3e are marked at 90% false alarm level. 40 min periodicity in IEFy can be seen to affect EEJ over India and vertical drift over Jicamarca as coherency is high and phase is stable at this periodicity. JRO = Jicamarca Radio Observatory.

−24 m/s at 0545 UT to −50 m/s at 0618 UT. The maximum change in drift is ~ −25 m/s during 0545–0618 UT. It is to be noted that the drift velocity of −25 m/s corresponds to a westward electric field of 0.5 mV/m over Jicamarca.

It is to be noted that while the downward drift ~0618 UT over Jicamarca is associated with the positive excursion of IEFy, the subsequent upward drift at ~0700 UT is associated with the negative excursion of IEFy. It is seen that IEFy remained steadily positive for about an hour before turning to negative direction. These observations suggest that the downward drift over Jicamarca ~0618 UT is due to westward PP electric field perturbation and the upward drift ~0700 UT is caused by the eastward OS electric field perturbation. The EEJ strength (in Figure 2f) shows a very good correlation with IEFy, and it is also quite different from the quiet day variations on 13 April 2013 (Ap = 6) during this period. Further, it is to be noted that the EEJ strength sharply

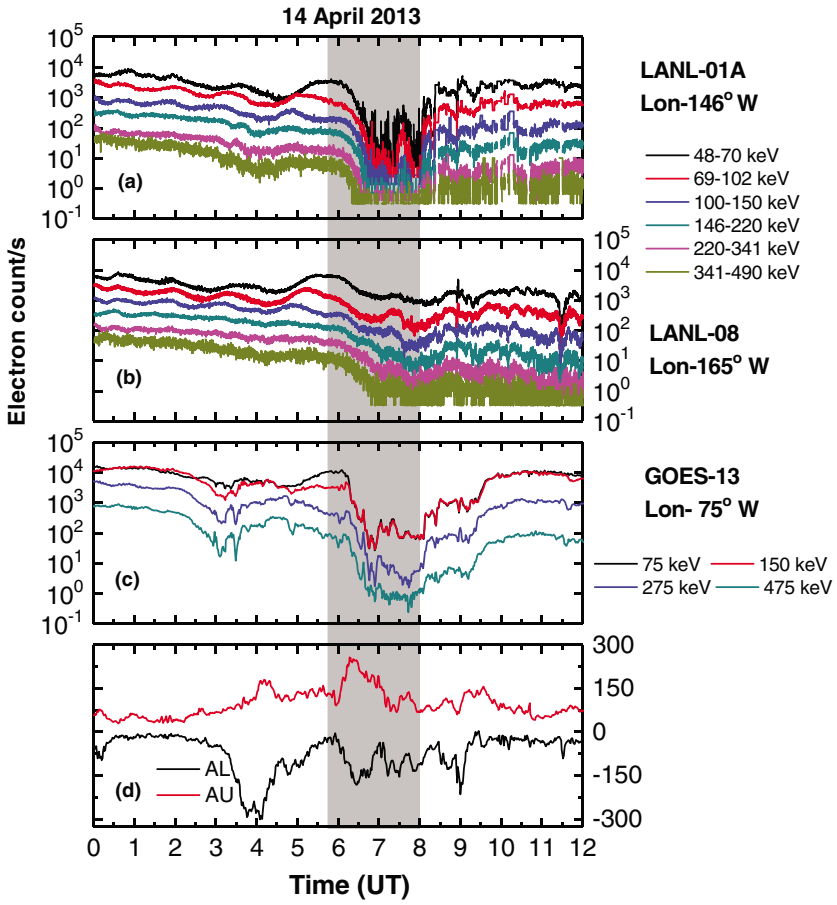

Figure 4. Electron injection data measured at geosynchronous orbit by (a) LANL-01A, (b) LANL-08, (c) GOES satellites, and (d) the eastward (AU index) and westward (AL index) auroral electrojet strength, during 0000–1200 UT (0512–1712 LT) on 14 April 2014. The energy channels of LANL and GOES satellites are mentioned in the right side of the corresponding figures. The gray shaded region (0545–0800 UT) marks the interval when the electric field perturbations are observed over Arecibo/Jicamarca and Indian sector. LANL = Los Alamos National Laboratory.

changed from 42 nT at 0545 to 84 nT at 0618 UT under the influence of eastward PP electric field. So the change in EEJ strength is 42 nT during this time. In addition, the subsequent sharp decrease in EEJ strength from ~65 nT at ~0630 UT to 11 nT at ~0712 UT under the influence of OS electric field is also seen. The variations in PC index and EEJ closely resemble with each other during this period. Interestingly, the variations in EEJ and vertical drifts over Jicamarca/Arecibo are out of phase with each other.

In order to bring out the periodic components in IEFy, EEJ, and vertical plasma drift during the passage of a sheath region, harmonic analyses were performed by using the standard algorithm by Schulz and Stattegger (1997). Figure 3 depicts the periodic components of (a) IEFy, (b) EEJ, and (c) vertical drift during the interval 0545–0800 UT. The fast fluctuating components are extracted by using the Savitzky and Golay (1964) smoothing algorithm. This technique helps to get the periodicities of smaller fluctuations. The dashed horizontal lines in Figures 3a–3c are marked at the significance level of 5% determined by Siegel's test (1980). Siegel's test calculates the significance level in such a way that multiple periodic components become "significant" in a power spectra. A confidence level of 95% (or 5% significance level) is equivalent to the $\pm 2\sigma$ level in the fast Fourier transform method. The choice of this confidence level decides the critical level of the Siegel-test statistics (Schulz & Stattegger, 1997). Periodicity of 40 min (marked by gray shaded box) is found to be significant and present in all the parameters. Further, to know the causal relationship between two time series at this given frequency, cross-spectrum analyses are performed. The squared coherency and phase spectra between IEFy and EEJ strength as well as IEFy and vertical drift are depicted in Figures 3d and 3e, respectively. The horizontal dashed line in Figures 3d and 3e are marked at 90% false alarm level. It is found that the 40-mininner

edge of the ring curren periodicities in EEJ and vertical drift are highly coherent with 40-min periodicity in IEFy and the phase is also stable around this period. This suggests that the 40-min periodic component in EEJ and vertical drift is due to corresponding variations in IEFy during the passage of the ICME sheath region.

In order to delineate the possible effects due to other sources such as substorms and its impact on equatorial ionosphere during the passage of the ICME sheath region, LANL and GOES data sets are investigated. Figure 4 shows the variations of electron injections (counts/s) measured at geosynchronous orbit by (a) LANL-01A, (b) LANL-08, and (c) GOES satellites, along with (d) the eastward (AU index) and westward (AL index) auroral electrojet index, during 0000–1200 UT on 14 April 2014. The energy channels of LANL and GOES-13 satellites are mentioned in the right side of the corresponding figures. The LANL-01A, LANL-08, and GOES-13 satellites were at the longitudes 146°W (LT = UT − 9.7 hr), 165°W (LT = UT − 11 hr), and 75°W (LT = UT − 5 hr), respectively. The gray shaded region (0545–0800 UT) marks the interval when the electric field perturbations are observed over Arecibo/Jicamarca and Indian sector. It can be observed that the electron flux count started decreasing at ∼0545 UT and continued for ∼1.5 hr, which is a typical signature of substorm growth phase. This was followed by a dispersionless electron injection at 0810 UT, which indicates towards the onset of an expansion phase of a substorm. This feature is more conspicuous in the longitude sector of LANL-01A and GOES-13 compared to the longitude sector of LANL-08. Interestingly, the strengths of auroral electrojets particularly AL did not show any significant change during this time. Further, it must be noted that though the growth phase of substorm falls during the interval (0545–0800 UT) where the penetration of IEF is observed, but the expansion phase lies clearly outside of the given interval. The implications of these results will be discussed in the ensuing section.

4. Discussion

A CME that erupted from the active region NOAA11719 on 11 April 2013 passed by Earth during 13–14 April 2013 (Vemareddy & Mishra, 2015). The present investigation brings out various aspects of ionospheric and magnetospheric effects during the passage of this sheath region. It is known that a geomagnetic storm can be induced by a sheath, the leading and trailing part of a MC (Wu & Lepping, 2002). However, in this case, neither the sheath nor the MC was able to cause significant depression in SYM-H so as to be attributed as a typical geomagnetic storm. It was further shown that the perpendicular shocks are more geoeffective than a parallel shock as the perpendicular shock front can compress the IMF more than the parallel one (Kataoka et al., 2005; Yue & Zong, 2011). In this case, the shock normal angle is found to be 60.5° (Oliveira & Raeder, 2015), that is, the shock is more quasi-perpendicular. Though the IP shock is more perpendicular, the absence of predominantly southward IMF Bz led to a condition wherein the ring current intensity did not increase in strength. The IMF Bz is predominantly northward during this event except for a small duration 0545–0800 UT on 14 April 2013 when IMF Bz took two distinct southward excursions. The enhancement in SYM-H at ∼22:50 UT on 13 April 2013 is caused by an overcompression by quasi-perpendicular shock during the passage of ICME. It is to be noted that the energy transfer from solar wind to magnetosphere depends on the rate and duration of magnetic reconnection process between the Earth and interplanetary magnetic field (IMF Bz or the dawn-dusk component of IEF; Dungey, 1961). Therefore, not only a perpendicular shock but also a southward IMF Bz inside the ICME is required to increase the ring current strength (Yue & Zong, 2011). As the sheath region is highly turbulent, the solar wind parameters, particularly IMF Bz, fluctuate very fast and as a consequence, the growth of ring current may get inhibited. In addition to the sheath region of ICME, the MC region is also dominated by northward IMF Bz in the present case. Therefore, the ICME sheath region or the MC did not cause any geomagnetic storm and make SYM-H to be restricted at −7 nT. However, the global ionospheric electric field is found to be affected during 0545–0800 UT when IMF Bz takes two southward excursions inside the sheath region.

The present investigation shows a strong evidence of PP electric field from high to low latitude ionosphere both in day and night sectors during the passage of ICME sheath. In this case, the PP electric field is mainly associated to DP2 type periodic perturbation over the dip equator, which can also be driven by an ICME sheath. The periodic perturbations of 40 min in IEFy are causally connected to EEJ and drift over low latitudes (see Figure 3). During the DP2 type events, the magnetometers show a coherent and similar magnetic variations from high to low latitude as the IP electric field penetrates from high to low latitude nearly simultaneously (Nishida, 1968; Yizengaw et al., 2016). It is to be noted that the ionospheric electric field was found

to oscillate east and westward corresponding to north and southward fluctuations in IMF Bz and the time scale of quasiperiodic fluctuations can range from half an hour to several hours (Chakrabarty et al., 2005; Kikuchi et al., 2000). A wide range of periodicities of 30–40 min (Kikuchi et al., 1996), 25–35 min (Hanumath Sastri et al., 2000), and 40 min (Chakrabarty et al., 2008, 2015) have been reported by earlier investigations by various measurements. Further, a recent investigation of Rout et al. (2017) revealed that periodicities of 30 and 60 min in IMF Bz affected the equatorial ionosphere during the corotating interaction region-driven geomagnetic storms. However, the penetration of 40-min periodic fluctuations in IEFy associated with sheath region of an ICME is brought out for the first time by the present investigation. In addition, it is also to be noticed that the polarity of PP electric field is westward (eastward) during night sector (day sector) when IMF Bz turns to southward during 0545–0800 UT.

Identical variations between PC index and EEJ strength (see the shaded interval in Figures 2b and 2f) during 0545–0800 UT on 14 April 2013 unambiguously suggest that the effects of PP electric field at polar region and equator are nearly simultaneous. It has been shown that the PC index (Troshichev & Andrezen, 1985) and IEFy are well correlated and the PC index can effectively be used as ionospheric polar electric field during geomagnetic disturbed time (Nagatsuma et al., 2000; Troshichev et al., 2000). The large change in EEJ strength (from ∼40 to ∼84 nT) at 0545 UT is caused by a strong eastward electric field perturbation in day sector. During this event (0545–0800 UT on 14 April 2013), Arecibo and Jicamarca stations were located in night sector whereas India was in day sector. The plasma dynamics over Arecibo is more complex than Jicamarca and India as the plasma drift can be influenced by meridional wind at Arecibo due to finite dip angle (45°). Although the very small temporal scale fluctuations are absent in vertical drift over Arecibo due to reduced data cadence (smoothing), the downward drift due to westward electric field perturbation during 0545–0800 UT associated with the sheath region of ICME is very clear (see Figure 2c). It is to be noted that the meridional wind velocity over Arecibo was in equatorial direction although the magnitude was relatively less (∼ −20 m/s). The equatorial wind would have moved the plasma upward, but the downward plasma drift at this time strongly indicates the clear influence of a westward electric field. In the present investigation, the polarities of PP electric field during day and nighttime are in agreement with earlier works by Nopper and Carovillano (1978) and Fejer et al. (2008). The westward polarity of PP electric field has also been observed by earlier studies at this local time over Arecibo (Buonsanto et al., 1999; Erickson et al., 2010), and these events were mainly associated with strong geomagnetic storms. Opposite polarities of PP electric field over Indian and Jicamarca sectors are also in accordance with the earlier results (Kelley et al., 2007).

Recently, it is discussed by Borovsky and Shprits (2017) that the Dst index may not be a good proxy to gauge the strength of a geomagnetic storm and its effects on near earth space environment. It is argued that Dst index fails to capture various processes in the magnetosphere-ionosphere system during geomagnetic storms that include ionospheric Joule heating, outflow, changes in the thermospheric density, particle precipitation, state of the radiation belts, the evolution of the hot-plasma ions and electrons in the magnetosphere, and also the geomagnetic storm time evolution of the cold plasma of the plasmasphere and plumes. In addition, it is also well known that the CIR-driven geomagnetic storms can cause significant changes in radiation belt (Tsurutani et al., 2006) and global ionosphere (Rout et al., 2017) though the strength of ring current (Dst index) is less. Therefore, it is not surprising that the geoeffectivenss of an ICME event, in which the IMF Bz polarity is northward inside the MC structure and it is fluctuating in the sheath region, may not be captured efficiently by Dst index. Under these circumstances, PP electric field perturbations can be taken as proxy to evaluate the geoeffectiveness.

The sheath regions are highly turbulent due to plasma instabilities and can trigger substorms on many occasions (Akasofu & Chao, 1980; Pulkkinen et al., 2007). However, during 0545–0800 UT, there was no onset of an expansion phase of a substorm. It is argued by Janzhura et al. (2007) that during substorm, the strength of AL index should exceed at least −400 nT. This is not the case here as AL did not exceed −400 nT. On the other hand, the high correlation between IEFy and other ionospheric electric field measurements strongly supports the arguments that the global ionospheric electric field is mainly driven by DP2 type electric field perturbations and not by substorms.

5. Summary

Based on the observations using multiple techniques, the present investigation brings out the following salient points:

1. The sheath region of ICME during this event passes 1 AU for a long duration (~18 hr), which is followed by an MC. The polarity of IMF Bz is northward inside the MC. SYM-H index does not capture the geoeffectiveness of this event as the minimum depression in SYM-H is restricted to −7 nT.
2. Interestingly, DP2 type quasiperiodic fluctuations of 40 min in the vertical drift are observed over Jicamarca and EEJ over Indian sector. It is shown for the first time that the DP2 type electric field perturbation over equatorial ionosphere can also be driven by a sheath region of ICME.
3. The polarity of PP electric field, associated with the sheath region of ICME is found to be westward over Jicamarca/Arecibo (night sector) and eastward over Indian sector (daytime) during 0545–0800 UT. The polarity of PP electric field corresponding to the local time observations are in agreement with the earlier works by Nopper and Carovillano (1978) and Fejer et al. (2008).
4. It is suggested that the PP electric field perturbations should be evaluated for geoeffectiveness of ICME when the polarity of IMF Bz is northward inside the MC region of the ICME.

Acknowledgments
Magnetic data from the three Indian stations (TIR and ABG) are provided by Indian Institute of Geomagnetism, India. The geomagnetic indices and solar wind data are obtained from NASA GSFC CDAWeb (http://cdaweb.gsfc.nasa.gov/). The plasma drift data over Jicamarca and Arecibo and meridional wind over Arecibo used in this work were taken from Madrigal Database at Jicamarca Radio Observatory (http://madrigal.naic.edu/). The Jicamarca Radio Observatory is a facility of the Instituto Geofisico del Peru operated with support from the NSFAGS-1433968 through Cornell University. The Arecibo Observatory is operated by SRI International under a cooperative agreement with the National Science Foundation (LT-1100968) and in alliance with Ana G. Mendez-Universidad Metropolitana and the Universities Space Research Association. The geosynchronous particle injection data are provided by Los Alamos National Laboratory, USA. This work is supported by the Department of Space, Government of India. The work at Utah State University was supported by the NASA H-LWS program through grant 80NSSC17K071.

References

Akasofu, S.-I., & Chao, J. (1980). Interplanetary shock waves and magnetospheric substorms. *Planetary and Space Science*, *28*(4), 381–385. https://doi.org/10.1016/0032-0633(80)90042-2

Borovsky, J. E., & Shprits, Y. (2017). Is the Dst index sufficient to define all geospace storms. *Journal of Geophysical Research: Space Physics*, *122*, 11,543–11,547. https://doi.org/10.1002/2017JA024679

Buonsanto, M., González, S., Pi, X., Ruohoniemi, J., Sulzer, M., Swartz, W., et al. (1999). Radar chain study of the May, 1995 storm. *Journal of Atmospheric and Terrestrial Physics*, *61*(3–4), 233–248. https://doi.org/10.1016/S1364-6826(98)00134-5

Burlaga, L. F., Klein, L., Sheeley, N. R., Michels, D. J., Howard, R. A., Koomen, M. J., et al. (1982). A magnetic cloud and a coronal mass ejection. *Geophysical Research Letters*, *9*(12), 1317–1320. https://doi.org/10.1029/GL009i012p01317

Chakrabarty, D., Rout, D., Sekar, R., Narayanan, R., Reeves, G. D., Pant, T. K., et al. (2015). Three different types of electric field disturbances affecting equatorial ionosphere during a long-duration prompt penetration event. *Journal of Geophysical Research: Space Physics*, *120*, 4993–5008. https://doi.org/10.1002/2014JA020759

Chakrabarty, D., Sekar, R., Narayanan, R., Devasia, C. V., & Pathan, B. M. (2005). Evidence for the interplanetary electric field effect on the OI 630.0 nm airglow over low latitude. *Journal of Geophysical Research*, *110*, A11301. https://doi.org/10.1029/2005JA011221

Chakrabarty, D., Sekar, R., Narayanan, R., Patra, A. K., & Devasia, C. V. (2006). Effects of interplanetary electric field on the development of an equatorial spread f event. *Journal of Geophysical Research*, *111*, A12316. https://doi.org/10.1029/2006JA011884

Chakrabarty, D., Sekar, R., Sastri, J. H., & Ravindran, S. (2008). Distinctive effects of interplanetary electric field and substorm on nighttime equatorial F layer: A case study. *Geophysical Research Letters*, *35*, L19108. https://doi.org/10.1029/2008GL035415

Dungey, J. W. (1961). Interplanetary magnetic field and the auroral zones. *Physical Review Letters*, *6*, 47–48. https://doi.org/10.1103/PhysRevLett.6.47

Echer, E., Gonzalez, W. D., Tsurutani, B. T., & Gonzalez, A. L. C. (2008). Interplanetary conditions causing intense geomagnetic storms (Dst ≤ -100 nt) during solar cycle 23 (1996–2006). *Journal of Geophysical Research*, *113*, A05221. https://doi.org/10.1029/2007JA012744

Erickson, P., Goncharenko, L., Nicolls, M., Ruohoniemi, M., & Kelley, M. (2010). Dynamics of North American sector ionospheric and thermospheric response during the November 2004 superstorm. *Journal of Atmospheric and Terrestrial Physics*, *72*(4), 292–301. https://doi.org/10.1016/j.jastp.2009.04.001

Fejer, B. G. (1993). F region plasma drifts over Arecibo: Solar cycle, seasonal, and magnetic activity effects. *Journal of Geophysical Research*, *98*(A8), 13,645–13,652. https://doi.org/10.1029/93JA00953

Fejer, B. G. (2011). Low latitude ionospheric electrodynamics. *Space Science Reviews*, *158*(1), 145–166. https://doi.org/10.1007/s11214-010-9690-7

Fejer, B. G., & Emmert, J. T. (2003). Low-latitude ionospheric disturbance electric field effects during the recovery phase of the 1921 October 1998 magnetic storm. *Journal of Geophysical Research*, *108*(A12), 1454. https://doi.org/10.1029/2003JA010190

Fejer, B. G., Jensen, J. W., & Su, S.-Y. (2008). Seasonal and longitudinal dependence of equatorial disturbance vertical plasma drifts. *Geophysical Research Letters*, *35*, L20106. https://doi.org/10.1029/2008GL035584

Gopalswamy, N., Akiyama, S., Yashiro, S., Michalek, G., & Lepping, R. (2008). Solar sources and geospace consequences of interplanetary magnetic clouds observed during solar cycle 23. *Journal of Atmospheric and Terrestrial Physics*, *70*(2–4), 245–253. https://doi.org/10.1016/j.jastp.2007.08.070

Guo, J., Feng, X., Zuo, P., Zhang, J., Wei, Y., & Zong, Q. (2011). Interplanetary drivers of ionospheric prompt penetration electric fields. *Journal of Atmospheric and Terrestrial Physics*, *73*(1), 130–136. https://doi.org/10.1016/j.jastp.2010.01.010

Hanumath Sastri, J., Luhr, H., Tachihara, H., Kitamura, T.-I., & Rao, J. V. S. V. (2000). Letter to the editor electric field fluctuations (25–35 min) in the midnight dip equatorial ionosphere. *Annales de Geophysique*, *18*(2), 252–256. https://doi.org/10.1007/s00585-000-0252-2

Huttunen, K. E. J., & Koskinen, H. E. J. (2004). Importance of post-shock streams and sheath region as drivers of intense magnetospheric storms and high-latitude activity. *Annales de Geophysique*, *22*(5), 1729–1738. https://doi.org/10.5194/angeo-22-1729-2004

Huttunen, K. E. J., Koskinen, H. E. J., Karinen, A., & Mursula, K. (2006). Asymmetric development of magnetospheric storms during magnetic clouds and sheath regions. *Geophysical Research Letters*, *33*, L06107. https://doi.org/10.1029/2005GL024894

Huttunen, K. E. J., Koskinen, H. E. J., & Schwenn, R. (2002). Variability of magnetospheric storms driven by different solar wind perturbations. *Journal of Geophysical Research*, *107*(A7), 1121. https://doi.org/10.1029/ 2001JA900171

Janzhura, A., Troshichev, O., & Stauning, P. (2007). Unified PC indices: Relation to isolated magnetic substorms. *Journal of Geophysical Research*, *112*, A09207. https://doi.org/10.1029/2006JA012132

Kataoka, R., Watari, S., Shimada, N., Shimazu, H., & Marubashi, K. (2005). Downstream structures of interplanetary fast shocks associated with coronal mass ejections. *Geophysical Research Letters*, *32*, L12103. https://doi.org/10.1029/2005GL022777

Kelley, M., Nicolls, M., Anderson, D., Anghel, A., Chau, J., Sekar, R., et al. (2007). Multi-longitude case studies comparing the interplanetary and equatorial ionospheric electric fields using an empirical model. *Journal of Atmospheric and Terrestrial Physics*, *69*(10–11), 1174–1181. https://doi.org/10.1016/j.jastp.2006.08.014

Kikuchi, T., Ebihara, Y., Hashimoto, K. K., Kataoka, R., Hori, T., Watari, S., & Nishitani, N. (2010). Penetration of the convection and overshielding electric fields to the equatorial ionosphere during a quasiperiodic DP 2 geomagnetic fluctuation event. *Journal of Geophysical Research*, *115*, A05209. https://doi.org/10.1029/2008JA013948

Kikuchi, T., Lühr, H., Kitamura, T., Saka, O., & Schlegel, K. (1996). Direct penetration of the polar electric field to the equator during a Dp 2 event as detected by the auroral and equatorial magnetometer chains and the EISCAT radar. *Journal of Geophysical Research*, *101*(A8), 17,161–17,173. https://doi.org/10.1029/96JA01299

Kikuchi, T., Lühr, H., Schlegel, K., Tachihara, H., Shinohara, M., & Kitamura, T.-I. (2000). Penetration of auroral electric fields to the equator during a substorm. *Journal of Geophysical Research*, *105*(A10), 23,251–23,261. https://doi.org/10.1029/2000JA900016

Lugaz, N., Farrugia, C. J., Winslow, R. M., Al-Haddad, N., Kilpua, E. K. J., & Riley, P. (2016). Factors affecting the geoeffectiveness of shocks and sheaths at 1 au. *Journal of Geophysical Research: Space Physics*, *121*, 10,861–10,879. https://doi.org/10.1002/2016JA023100

Manchester, W. B., Gombosi, T. I., Zeeuw, D. L. D., Sokolov, I. V., Roussev, I. I., Powell, K. G., et al. (2005). Coronal mass ejection shock and sheath structures relevant to particle acceleration. *The Astrophysical Journal*, *622*(2), 1225.

Nagatsuma, T., Obara, T., & Ishibashi, H. (2000). Relationship between solar wind parameters and magnetic activity in the near-pole region: Application to space weather forecasting. *Advances in Space Research*, *26*(1), 103–106. https://doi.org/10.1016/S0273-1177(99)01033-9

Nishida, A. (1968). Geomagnetic DP 2 fluctuations and associated magnetospheric phenomena. *Journal of Geophysical Research*, *73*(5), 1795–1803. https://doi.org/10.1029/JA073i005p01795

Nopper, R. W., & Carovillano, R. L. (1978). Polar-equatorial coupling during magnetically active periods. *Geophysical Research Letters*, *5*(8), 699–702. https://doi.org/10.1029/GL005i008p00699

Oliveira, D. M., & Raeder, J. (2015). Impact angle control of interplanetary shock geoeffectiveness: A statistical study. *Journal of Geophysical Research: Space Physics*, *120*, 4313–4323. https://doi.org/10.1002/2015JA021147

Pulkkinen, T. I., Partamies, N., Huttunen, K. E. J., Reeves, G. D., & Koskinen, H. E. J. (2007). Differences in geomagnetic storms driven by magnetic clouds and icme sheath regions. *Geophysical Research Letters*, *34*, L02105. https://doi.org/10.1029/2006GL027775

Rastogi, R., & Patil, A. (1986). Complex structure of equatorial electrojet current. *Current Science*, *55*(9), 433–436.

Rout, D., Chakrabarty, D., Janardhan, P., Sekar, R., Maniya, V., & Pandey, K. (2017). Solar wind flow angle and geoeffectiveness of corotating interaction regions: First results. *Geophysical Research Letters*, *44*, 4532–4539. https://doi.org/10.1002/2017GL073038

Savitzky, A., & Golay, M. J. (1964). Smoothing and differentiation of data by simplified least squares procedures. *Analytical Chemistry*, *36*(8), 1627–1639. https://doi.org/10.1021/ac60214a047

Scherliess, L., & Fejer, B. G. (1999). Radar and satellite global equatorial f region vertical drift model. *Journal of Geophysical Research*, *104*(A4), 6829–6842. https://doi.org/10.1029/1999JA900025

Schulz, M., & Stattegger, K. (1997). SPECTRUM: Spectral analysis of unevenly spaced paleoclimatic time series. *Computers & Geosciences*, *23*(9), 929–945. https://doi.org/10.1016/S0098-3004(97)00087-3

Senior, C., & Blanc, M. (1984). On the control of magnetospheric convection by the spatial distribution of ionospheric conductivities. *Journal of Geophysical Research*, *89*(A1), 261–284. https://doi.org/10.1029/JA089iA01p00261

Siegel, A. F. (1980). Testing for periodicity in a time series. *Journal of the American Statistical Association*, *75*(370), 345–348.

Simi, K. G., Thampi, S. V., Chakrabarty, D., Pathan, B. M., Prabhakaran Nayar, S. R., & Kumar Pant, T. (2012). Extreme changes in the equatorial electrojet under the influence of interplanetary electric field and the associated modification in the low-latitude f region plasma distribution. *Journal of Geophysical Research*, *117*, A03331. https://doi.org/10.1029/2011JA017328

Sulzer, M. P., Aponte, N., & González, S. A. (2005). Application of linear regularization methods to Arecibo vector velocities. *Journal of Geophysical Research*, *110*, A10305. https://doi.org/10.1029/2005JA011042

Troshichev, O., & Andrezen, V. (1985). The relationship between interplanetary quantities and magnetic activity in the southern polar cap. *Planetary and Space Science*, *33*(4), 415–419. https://doi.org/10.1016/0032-0633(85) 90086-8

Troshichev, O. A., Lukianova, R. Y., Papitashvili, V. O., Rich, F. J., & Rasmussen, O. (2000). Polar cap index (PC) as a proxy for ionospheric electric field in the near-pole region. *Geophysical Research Letters*, *27*(23), 3809–3812. https://doi.org/10.1029/2000GL003756

Tsurutani, B. T., Gonzalez, W. D., Gonzalez, A. L. C., Guarnieri, F. L., Gopalswamy, N., Grande, M., et al. (2006). Corotating solar wind streams and recurrent geomagnetic activity: A review. *Journal of Geophysical Research*, *111*, A07S01. https://doi.org/10.1029/2005JA011273

Tsurutani, B. T., Gonzalez, W. D., Tang, F., Akasofu, S. I., & Smith, E. J. (1988). Origin of interplanetary southward magnetic fields responsible for major magnetic storms near solar maximum (1978-1979). *Journal of Geophysical Research*, *93*(A8), 8519–8531. https://doi.org/10.1029/JA093iA08p08519

Vemareddy, P., & Mishra, W. (2015). A full study on the Sun–Earth connection of an earth-directed CME magnetic flux rope. *The Astrophysical Journal*, *814*(1), 59.

Wei, Y., Hong, M., Pu, Z., Zong, Q.-G., Nagai, T., Cao, X., et al. (2011). Responses of the ionospheric electric field to the sheath region of ICME: A case study. *Journal of Atmospheric and Terrestrial Physics*, *73*(1), 123–129. https://doi.org/10.1016/j.jastp.2010.03.004

Wu, C.-C., & Lepping, R. P. (2002). Effects of magnetic clouds on the occurrence of geomagnetic storms: The first 4 years of Wind. *Journal of Geophysical Research*, *107*(A10), 1314. https://doi.org/10.1029/2001JA000161

Yizengaw, E., Moldwin, M. B., Zesta, E., Magoun, M., Pradipta, R., Biouele, C. M., et al. (2016). Response of the equatorial ionosphere to the geomagnetic DP 2 current system. *Geophysical Research Letters*, *43*, 7364–7372. https://doi.org/10.1002/2016GL070090

Yue, C., & Zong, Q. (2011). Solar wind parameters and geomagnetic indices for four different interplanetary shock/ICME structures. *Journal of Geophysical Research*, *116*, A12201. https://doi.org/10.1029/2011JA017013

Zurbuchen, T. H., & Richardson, I. G. (2006). In-situ solar wind and magnetic field signatures of interplanetary coronal mass ejections. In *Coronal Mass Ejections, Space Sciences Series of ISSI* (Vol. 21, pp. 31–43). New York: Springer. https://doi.org/10.1007/978-0-387-45088-9-3